EUROPEAN ORGANIZATION FOR NUCLEAR RESEARCH

CERN–PPE/95–49
11 April 1995

# Evidence for gluon interference in hadronic Z decays

**The L3 Collaboration**

**ABSTRACT**

We present evidence for soft gluon interference, as required by QCD. This interference is expected to manifest itself in an angular ordering of the gluons radiated within a jet. Using hadronic decays of the Z boson in the L3 detector at LEP, we compare variables sensitive to such an angular ordering, namely the energy-energy correlation asymmetry and the newly introduced particle-particle correlation asymmetry, with the predictions of various parton shower models. Only those models which incorporate the expected interference agree with the data.

Submitted to *Physics Letters B*

# Introduction

Within the framework of QCD [1], the evolution into jets of a quark-antiquark pair produced in Z decay is usually described in two stages. The first stage is perturbative and proceeds via the radiation of gluons, which in turn radiate further gluons or split into $q\overline{q}$ pairs. QCD requires that this parton radiation be coherent, which results in interference both between gluons radiated from the same parton and between gluons radiated from different partons [2].

Due to the non-Abelian nature of QCD, the overall result of this interference is "angular ordering" of the gluon radiation [3], which constrains the angles between the radiator and the radiated gluon to decrease as the evolution proceeds to lower energy scales (and to later times). This can be understood qualitatively [2] by noting that as the energy of the radiated gluon decreases and/or its angle increases, the gluon probes a larger (transverse) spatial region. This leads to "colour screening", as soft gluons tend to experience the average colour charge of several branches, which is in general smaller than that of the radiator itself.

The parton shower is followed by the hadronization stage. Despite the essentially non-perturbative character of this stage it has been suggested, using the concept of Local Parton Hadron Duality (LPHD) [4], that many distributions of hadrons rather closely follow the corresponding parton distribution, with non-perturbative effects affecting mainly the normalization rather than the shape of the distributions.

To calculate effects of QCD, we turn to Monte Carlo methods. As is well known, the parton shower evolution picture is particularly well suited to such techniques, where a specific probability is assigned to each type of parton branching [5]. Although in this way leading logarithmic terms are summed to all orders, resulting in generally accurate predictions, gluon interference phenomena are usually not taken directly into account as the evolution of each quark is treated independently. In most models gluon interference is imposed as an *a posteriori* constraint forcing angular ordering of the gluon emitted in the shower. This is the case in JETSET PS [6] and HERWIG [7], which subsequently implement the non-perturbative step using string and cluster fragmentation, respectively. In JETSET the angular-ordering constraint can be turned off. The ARIADNE generator [8], on the other hand, produces the parton shower as a consequence of dipole radiation, by treating each $q\overline{q}$ or qg pair as a colour dipole which can radiate a gluon. This formulation naturally incorporates interference phenomena. Subsequent fragmentation is performed by string fragmentation as in JETSET. On the other hand, independent fragmentation models such as COJETS [9] implement the parton shower without including gluon coherence.

Fixed-order perturbative calculations, *e.g.*, the JETSET ME incorporation of second-order matrix elements [10], are well suited to study leading parton behaviour. But, given the small number of partons generated, they are not expected to reproduce soft gluon interference effects.

Gluon interference is expected to manifest itself in two regimes in Z hadronic decays [2]. In one case it affects the region between jets (interjet region). There it can explain [11], as a purely perturbative effect at the parton level, the so-called string effect, first predicted by string fragmentation phenomenology [12] and later discovered by the JADE experiment [13]. A detailed study of this aspect is the subject of our recent paper [14]. In the second case, gluon coherence affects the region within a jet (intrajet region). This results, *e.g.*, in suppression of hadrons with low momenta. This theoretical prediction is supported by many experiments (see, *e.g.*, our study [15]). In the present paper we study the effects of gluon coherence without making the (somewhat artificial) distinction between two- and three-jet events.

The angular ordering of the partons is expected, through LPHD, to be detectable in the final state hadrons. This suggests that we examine variables based on the angles between particles. Two-particle azimuthal correlations have been studied by OPAL [16]. In this paper we study two-particle correlations in the full spatial angle using data obtained with the L3 detector at LEP. A well-known angular correlation is the energy-energy correlation (EEC) [17]:

$$\mathrm{EEC}(\chi) = \frac{1}{N_{\mathrm{ev}}} \frac{1}{\Delta\chi} \sum_{1}^{N_{\mathrm{ev}}} \sum_{i=1}^{N_{\mathrm{ch}}} \sum_{\substack{j=1 \\ j\neq i}}^{N_{\mathrm{ch}}} \frac{E_i E_j}{E_{\mathrm{vis}}^2}\, \delta_{\mathrm{bin}}(\chi - \chi_{ij})$$

where $\chi_{ij}$ is the angle between tracks $i$ and $j$, $N_{\mathrm{ev}}$ is the number of events, $\Delta\chi$ is the bin width, $N_{\mathrm{ch}}$ is the number of charged tracks in an event, $E_i$ is the energy of track $i$, $E_{\mathrm{vis}} = \sum_{i=1}^{N_{\mathrm{ch}}} E_i$, and $\delta_{\mathrm{bin}}(\chi - \chi_{ij})$ is 1 if $\chi_{ij}$ and $\chi$ are in the same bin and 0 otherwise.

The energy weighting makes the EEC "infra-red safe" [17], hence reliably calculable. This is the reason it and its asymmetry (EECA)

$$\mathrm{EECA}(\chi) = \mathrm{EEC}(180^\circ - \chi) - \mathrm{EEC}(\chi)$$

have proved so useful in measuring quantities of perturbative QCD such as the strong coupling constant. However, the resulting emphasis on the most energetic branchings, may be undesirable for the purpose of investigating the extent of angular ordering. We therefore also examine analogously defined variables where the energy weighting is removed:

$$\begin{aligned}
\mathrm{PPC}(\chi) &= \frac{1}{N_{\mathrm{ev}}} \frac{1}{\Delta\chi} \sum_{1}^{N_{\mathrm{ev}}} \sum_{i=1}^{N_{\mathrm{ch}}} \sum_{\substack{j=1 \\ j\neq i}}^{N_{\mathrm{ch}}} \frac{1}{N_{\mathrm{ch}}^2}\, \delta_{\mathrm{bin}}(\chi - \chi_{ij}) \\
\mathrm{PPCA}(\chi) &= \mathrm{PPC}(180^\circ - \chi) - \mathrm{PPC}(\chi)
\end{aligned}$$

We call these variables the particle-particle correlation (PPC) and its asymmetry (PPCA).

At $\sqrt{s} = M_{\mathrm{Z}}$, the fraction of two-jet events is high. In such events particles in different jets will in general be separated by an angle $\chi$ greater than 90°. The EEC (PPC) for $\chi > 90^\circ$ can therefore serve as an indication of what the EEC (PPC) *within* a jet ($\chi < 90^\circ$) would be *in the absence of* angular ordering (or other short-range angular correlations). By forming the asymmetry, these "uninteresting" correlations are effectively subtracted. Also, some cancellation of non-perturbative hadronization effects as well as some detector effects and Monte Carlo uncertainties [18] can be expected. On the other hand, three-jet events will produce large negative values of PPCA and EECA at small $\chi$ since there is no directly opposite jet. Nevertheless, we prefer to make no distinction between two- and three-jet events since jet algorithms introduce additional systematic uncertainties.

# The L3 detector

The L3 detector [19] consists of a central tracking chamber, a high resolution electromagnetic calorimeter composed of bismuth germanium oxide crystals, a ring of scintillation counters, a uranium and brass hadron calorimeter with proportional wire chamber readout, and an accurate muon chamber system. These detectors are installed in a 12 m diameter magnet which provides a uniform field of 0.5 T along the beam direction.

To calculate the angular correlations, only tracks in the central tracking chamber have been used. The angular resolution for pairs of tracks is better than 0.7° [20]. For the energy-energy correlation measurements, the momentum of tracks measured in the tracking chamber is used rather than the calorimeter energy.

# Data Selection

Events collected by L3 at a centre of mass energy of $\sqrt{s} = 91.2$ GeV during the 1992 LEP running period, corresponding to 654k hadronic Z decays, are used for this analysis. The combined trigger efficiency for hadronic events exceeds 99.95% [21].

Events are selected in two steps. In the first step, hadronic events are selected using the energy measured in the electromagnetic and hadronic calorimeters with the requirements:

$$0.6 < \frac{E_{\rm vis}^{\rm cal}}{\sqrt{s}} < 1.4, \qquad \frac{|E_{\parallel}^{\rm cal}|}{E_{\rm vis}^{\rm cal}} < 0.4, \qquad \frac{E_{\perp}^{\rm cal}}{E_{\rm vis}^{\rm cal}} < 0.4, \ \text{and} \qquad N_{\rm cluster}^{\rm cal} > 12,$$

where $E_{\rm vis}^{\rm cal}$ is the total energy observed in the calorimeters, $E_{\parallel}^{\rm cal}$ and $E_{\perp}^{\rm cal}$ are the energy imbalances along and transverse to the beam direction, respectively, and $N_{\rm cluster}^{\rm cal}$ is the number of calorimeter clusters. Calorimeter clusters are found by combining calorimeter signals from neighbouring cells when it is likely that they have been caused by a single particle. Only clusters with an energy greater than 100 MeV are used. Since the number of clusters is proportional to the number of particles in the event, the cut on $N_{\rm cluster}^{\rm cal}$ serves to reject low multiplicity events, which are mainly non-hadronic. Applying these cuts to fully simulated events, we find that 98% of the hadronic events are accepted. As we use only charged tracks in the analysis, we require in addition that the direction of the event thrust be within the full acceptance of the central tracking chamber ($45° < \theta < 135°$).

In the second step, events are selected from the above-described hadronic sample using tracks which have passed certain quality criteria. The distance of closest approach of the tracks to the interaction point is required to be less than 20 mm and the momentum measured in the plane transverse to the beam direction is required to be more than 100 MeV/$c$. Events are then selected using criteria similar to the above calorimeter-based selection but using tracks:

$$0.3 < \frac{\sum |p|}{\sqrt{s}}, \qquad \frac{\sum |p_{\parallel}|}{\sum |p|} < 0.75, \qquad \frac{|\sum \vec{p_{\perp}}|}{\sum |p|} < 0.75, \ \text{and} \qquad N_{\rm ch} > 4,$$

where $p$ is the track momentum. The resulting sample contains about 377k events.

# Results

Our results on the EECA and PPCA are compared with several Monte Carlo generators used to simulate the reaction $e^+e^- \rightarrow q\overline{q}$ with subsequent quark and gluon branchings (parton showers). For our purpose these models can be divided into two categories: those which do and those which do not incorporate colour coherence effects. Those which include coherence effects are HERWIG 5.6, JETSET 7.3 PS and ARIADNE 4.04, while JETSET 7.3 PS with the angular ordering option turned off and COJETS 6.23 do not. We also make a comparison with the matrix element implementation of JETSET, JETSET 7.3 ME. These programs have been briefly described in the introduction. They have all been tuned [22] to describe various one-dimensional distributions of our data, with the exception of JETSET PS with angular ordering turned off. For this model the average charged multiplicity is about 0.8 tracks too high when the parameter values of the angular ordered JETSET are used. This difference is removed by a change of less than one standard deviation in the tuned parameters while still preserving good agreement with the other distributions.

To calculate the correlations, we use charged particles from the selected data sample described above. We use a bin size of 6°, which is much larger than our resolution for the angle in space between two tracks. Such a large bin size simplifies the correction of the data for detector effects while still being small enough to study the effects of coherence.

Before comparing the EECA and PPCA of the data with the predictions of the coherent and incoherent models, we correct the data for detector efficiency and resolution and investigate the sensitivity of the correlations to uncertainties of the models, in particular to variations of the parameters of the models.

The corrections to the data are found using ~346k events generated using JETSET PS, fully simulated and reconstructed in the L3 detector. The option of angular ordering in parton showers was used to generate these events. An additive correction is calculated for each bin of the PPCA and EECA as the difference between the PPCA(EECA) calculated at generator level and that calculated using the full detector simulation (after event selection). The PPC and EEC distributions are corrected by a multiplicative factor determined from the ratio of the generator level and simulation level values. As a check, the corrections were also determined using HERWIG. The PPC and EEC distributions, using both corrections, are shown in Figure 1. The differences between the JETSET and HERWIG corrections are seen to be small. The corrections to the PPCA and EECA vary smoothly with $\chi$. In the region where the differences between the coherent and incoherent models are largest, namely $\sim 6-40°$, the corrections are smaller than 0.01 and 0.06 for the PPCA and EECA, respectively.

To investigate the sensitivity of the EECA and PPCA to various parameters of the models, the parameters of JETSET which were tuned by L3 were varied* by one standard deviation from their tuned values [22]. The results are shown in Figures 2a and 2c where the points represent the values found using the tuned values and lines indicate the maximum and minimum values found in the parameter variations. From Figure 2a

*The parameters varied are the scale $\Lambda_{LL}$, the width of the Gaussian transverse momentum distribution of the primary quarks $\sigma_q$, and the $b$ parameter in the symmetric Lund fragmentation function [23]. The JETSET default value of the shower cut-off parameter, 1 GeV, was used.

we conclude that there is a large difference in the PPCA in the region below about 54° between JETSET with and without angular ordering and that this difference is only slightly affected by reasonable variations of the JETSET parameters. A similar conclusion is reached for the EECA (Figure 2c), although for a narrower angular range. The sensitivity of the correlation asymmetries to resonance production was investigated by varying the vector/pseudoscalar ratio in JETSET.[†] Decreasing this ratio to 1/3 or increasing it to 3 produced changes in the correlation asymmetries comparable to those shown for the variation of the other model parameters. Thus mistuning of these parameters also cannot account for the differences seen between JETSET with and without angular ordering.

At small angles between particles we can expect the EEC and PPC to be strongly influenced by Bose-Einstein correlations and non-perturbative effects. This is also the region where the detector effects are most pronounced and least well understood. Therefore any differences observed at small angles are difficult to interpret. Unfortunately, the Bose-Einstein effect affects the correlations also at larger angles. This comes about partly through the normalization of the EEC and PPC, whereby a decrease in the small-$\chi$ bins must be compensated for by an increase in the other bins, but also directly, particularly for the PPC. This is because the Bose-Einstein effect is large for small $Q^2$. For two particles, $Q^2_{ij} = (p_i + p_j)^2 \approx 2E_iE_j(1 - \cos\chi_{ij})$. Thus, the larger the energies, the smaller $\chi$ must be to produce a large Bose-Einstein effect. Consequently, the influence of the Bose-Einstein effect is confined to small angles for the EECA, but less so for the PPCA. However, the shape of the distribution is largely unaffected, as may be seen in Figures 2b and 2d, where the PPCA, as well as the EECA, found using JETSET[‡] is shown with and without inclusion of the Bose-Einstein effect. We see that inclusion of the Bose-Einstein effect, as parametrized in JETSET, results in lower values of the PPCA for all values of $\chi$ irrespective of angular ordering. For the EECA, the Bose-Einstein effect is small for $\chi > 6°$.

We have identified two main sources of systematic error: (a) uncertainties in the values of Monte Carlo model parameters, for which we take as error the root-mean-square of the variations found from varying selected parameters (Figures 2a and 2b); and (b) uncertainties in the corrections for detector effects. The difference between the corrections using JETSET and those using HERWIG is taken as the systematic error. This is the dominant uncertainty in the analysis.

The models show the most striking difference in the region $\chi \leq 36°$ for the EECA and $\chi \leq 54°$ for the PPCA. We therefore direct our interest primarily to these regions, excluding the first bin, where both the Bose-Einstein effect and the detector corrections are largest.

Figures 3 and 4 show the PPCA and EECA distributions, respectively, of the corrected data compared with those of the coherent and the incoherent Monte Carlo models. We first discuss the comparison of the PPCA. We see that below 54° JETSET without

[†] The JETSET parameters PARJ(11), PARJ(12), and PARJ(13) for light, strange and heavy mesons, respectively, have as default values for this ratio 1, 1.5 and 3.

[‡] JETSET includes a parametrization of the Bose-Einstein effect in its fragmentation. ARIADNE uses JETSET for fragmentation and thus includes the same parametrization. We have used the Gaussian parametrization in JETSET with parameters PARJ(92)=1.5 and PARJ(93)=0.33. HERWIG and COJETS contain no treatment of the Bose-Einstein effect.

angular ordering disagrees strongly with the data, while being in fair agreement at larger values of $\chi$. COJETS is seen not to reproduce the data over the entire angular range, although the shape of its distribution is rather similar to that of the data. On the other hand, the coherent Monte Carlo models: JETSET with angular ordering, HERWIG, and ARIADNE, all reproduce the data reasonably well over the full angular range. Note that the disagreement of the non-angular ordered models can not be due to the Bose-Einstein effect. Turning this effect off in the non-angular ordered JETSET model (see Figure 2b) does not raise its PPCA points enough. Based on the behaviour of the Bose-Einstein effect in JETSET, we expect that its inclusion in COJETS would lower the COJETS points, putting them even further away from the data. We have attempted, without success, to improve the agreement with the PPCA and EECA by varying some of the parameters of COJETS. The failure of COJETS is perhaps not surprising since it has previously been found [22, 14] to be incapable of satisfactorily reproducing variables sensitive to transverse momentum spectra.

The comparison of the EECA leads to conclusions similar to those for the PPCA except that HERWIG compares here significantly worse than do angular ordered JETSET and ARIADNE.

We note that the matrix element version of JETSET agrees satisfactorily with our data for the EECA but not for the PPCA. Since the PPCA is much more sensitive to soft particles than is the EECA, this suggests that the disagreement arises from multiple soft gluon emission, which is not included in the matrix element calculation.

# Conclusions

We have studied gluon interference in hadronic Z decays using two correlations, the particle-particle correlation asymmetry (PPCA) and energy-energy correlation asymmetry (EECA). Striking differences are found between parton shower models which incorporate colour coherence and those which do not. The EECA is most sensitive to the most energetic branchings in the shower, whereas the PPCA is sensitive to branchings of all energies. While the PPCA is more influenced by the Bose-Einstein effect and other non-perturbative effects, the EECA is more sensitive to systematic uncertainties in the unfolding of detector effects. Both correlation asymmetries lead to the same conclusion: The data are generally in agreement with coherent models and strongly disfavour the incoherent models.

# Acknowledgements

We wish to express our gratitude to the CERN accelerator divisions for the excellent performance of LEP. We also acknowledge the efforts of all the engineers and technicians who have contributed to the construction and maintenance of this experiment.

We are grateful to T. Sjöstrand and P. Nason for elucidating discussions.

## The L3 Collaboration:


M.Acciarri[26] A.Adam[43] O.Adriani[16] M.Aguilar-Benitez[25] S.Ahlen[10] B.Alpat[33] J.Alcaraz[25] J.Allaby[17] A.Aloisio[28] G.Alverson[11] M.G.Alviggi[28] G.Ambrosi[33] Q.An[18] H.Anderhub[46] V.P.Andreev[37] T.Angelescu[12] D.Antreasyan[8] A.Arefiev[27] T.Azemoon[3] T.Aziz[9] P.V.K.S.Baba[18] P.Bagnaia[36,17] L.Baksay[42] R.C.Ball[3] S.Banerjee[9] K.Banicz[43] R.Barillère[17] L.Barone[36] P.Bartalini[33] A.Baschirotto[26] M.Basile[8] R.Battiston[33] A.Bay[22] F.Becattini[16] U.Becker[15] F.Behner[46] Gy.L.Bencze[13] J.Berdugo[25] P.Berges[15] B.Bertucci[17] B.L.Betev[46] M.Biasini[33] A.Biland[46] G.M.Bilei[33] R.Bizzarri[36] J.J.Blaising[17] G.J.Bobbink[2] R.Bock[1] A.Böhm[1] B.Borgia[36] A.Boucham[4] D.Bourilkov[46] M.Bourquin[19] D.Boutigny[4] B.Bouwens[2] E.Brambilla[15] J.G.Branson[38] V.Brigljevic[46] I.C.Brock[34] A.Bujak[43] J.D.Burger[15] W.J.Burger[19] C.Burgos[25] J.Busenitz[42] A.Buytenhuijs[30] X.D.Cai[18] M.Capell[15] G.Cara Romeo[8] M.Caria[33] G.Carlino[28] A.M.Cartacci[16] J.Casaus[25] G.Castellini[16] R.Castello[26] N.Cavallo[28] C.Cecchi[19] M.Cerrada[25] F.Cesaroni[36] M.Chamizo[25] A.Chan[48] Y.H.Chang[48] U.K.Chaturvedi[18] M.Chemarin[24] A.Chen[48] C.Chen[6] G.Chen[6] G.M.Chen[6] H.F.Chen[20] H.S.Chen[6] M.Chen[15] G.Chiefari[28] C.Y.Chien[5] M.T.Choi[41] L.Cifarelli[8] F.Cindolo[8] C.Civinini[16] I.Clare[15] R.Clare[15] T.E.Coan[23] H.O.Cohn[31] G.Coignet[4] N.Colino[17] V.Commichau[1] S.Costantini[36] F.Cotorobai[12] B.de la Cruz[25] X.T.Cui[18] X.Y.Cui[18] T.S.Dai[15] R.D'Alessandro[16] R.de Asmundis[28] H.De Boeck[30] A.Degré[4] K.Deiters[44] E.Dénes[13] P.Denes[35] F.DeNotaristefani[36] D.DiBitonto[42] M.Diemoz[36] C.Dionisi[36] M.Dittmar[46] A.Dominguez[38] A.Doria[28] I.Dorne[4] M.T.Dova[18,♯] E.Drago[28] D.Duchesneau[17] F.Duhem[4] P.Duinker[2] I.Duran[39] S.Dutta[9] S.Easo[33] Yu.Efremenko[31] H.El Mamouni[24] A.Engler[34] F.J.Eppling[15] F.C.Erné[2] J.P.Ernenwein[24] P.Extermann[19] R.Fabbretti[44] M.Fabre[44] R.Faccini[36] S.Falciano[36] A.Favara[16] J.Fay[24] M.Felcini[46] T.Ferguson[34] D.Fernandez[25] G.Fernandez[25] F.Ferroni[36] H.Fesefeldt[1] E.Fiandrini[33] J.H.Field[19] F.Filthaut[34] P.H.Fisher[15] G.Forconi[15] L.Fredj[19] K.Freudenreich[46] M.Gailloud[22] Yu.Galaktionov[27,15] S.N.Ganguli[9] P.Garcia-Abia[25] S.S.Gau[11] S.Gentile[36] J.Gerald[5] N.Gheordanescu[12] S.Giagu[36] S.Goldfarb[22] J.Goldstein[10] Z.F.Gong[20] E.Gonzalez[25] A.Gougas[5] D.Goujon[19] G.Gratta[32] M.W.Gruenewald[7] C.Gu[18] M.Guanziroli[18] V.K.Gupta[35] A.Gurtu[9] H.R.Gustafson[3] L.J.Gutay[43] B.Hartmann[1] A.Hasan[29] J.T.He[6] T.Hebbeker[7] A.Hervé[17] K.Hilgers[1] W.C.van Hoek[30] H.Hofer[46] H.Hoorani[19] S.R.Hou[48] G.Hu[18] M.M.Ilyas[18] V.Innocente[17] H.Janssen[4] B.N.Jin[6] L.W.Jones[3] P.de Jong[15] I.Josa-Mutuberria[25] A.Kasser[22] R.A.Khan[18] Yu.Kamyshkov[31] P.Kapinos[45] J.S.Kapustinsky[23] Y.Karyotakis[4] M.Kaur[18] S.Khokhar[18] M.N.Kienzle-Focacci[19] D.Kim[5] J.K.Kim[41] S.C.Kim[41] Y.G.Kim[41] W.W.Kinnison[23] A.Kirkby[32] D.Kirkby[32] J.Kirkby[17] S.Kirsch[45] W.Kittel[30] A.Klimentov[15,27] A.C.König[30] E.Koffeman[2] O.Kornadt[1] V.Koutsenko[15,27] A.Koulbardis[37] R.W.Kraemer[34] T.Kramer[15] W.Krenz[1] H.Kuijten[30] A.Kunin[15,27] P.Ladron de Guevara[25] G.Landi[16] M.Lanfranchi[33] C.Lapoint[15] K.Lassila-Perini[46] P.Laurikainen[21] M.Lebeau[17] A.Lebedev[15] P.Lebrun[24] P.Lecomte[46] J.Lecoq[4] P.Lecoq[17] P.Le Coultre[46] J.S.Lee[41] K.Y.Lee[41] I.Leedom[11] C.Leggett[3] J.M.Le Goff[17] R.Leiste[45] M.Lenti[16] E.Leonardi[36] P.Levtchenko[37] C.Li[20,18] E.Lieb[45] W.T.Lin[48] F.L.Linde[2] B.Lindemann[1] L.Lista[28] Y.Liu[18] Z.A.Liu[6] W.Lohmann[45] E.Longo[36] W.Lu[32] Y.S.Lu[6] K.Lübelsmeyer[1] C.Luci[36] D.Luckey[15] L.Ludovici[36] L.Luminari[36] W.Lustermann[44] W.G.Ma[20] A.Macchiolo[16] M.Maity[9] L.Malgeri[36] R.Malik[18] A.Malinin[27] C.Maña[25] S.Mangla[9] M.Maolinbay[46] P.Marchesini[46] A.Marin[10] J.P.Martin[24] F.Marzano[36] G.G.G.Massaro[2] K.Mazumdar[9] D.McNally[17] S.Mele[28] M.Merk[34] L.Merola[28] M.Meschini[16] W.J.Metzger[30] Y.Mi[22] A.Mihul[12] A.J.W.van Mil[30] Y.Mir[18] G.Mirabelli[36] J.Mnich[17] M.Möller[1] V.Monaco[36] B.Monteleoni[16] R.Moore[3] R.Morand[4] S.Morganti[36] N.E.Moulai[18] R.Mount[32] S.Müller[1] E.Nagy[13] S.Nahn[15] M.Napolitano[28] F.Nessi-Tedaldi[46] H.Newman[32] M.A.Niaz[18] A.Nippe[1] H.Nowak[45] G.Organtini[36] R.Ostonen[21] D.Pandoulas[1] S.Paoletti[36] P.Paolucci[28] G.Pascale[36] G.Passaleva[16] S.Patricelli[28] T.Paul[33] M.Pauluzzi[33] C.Paus[1] F.Pauss[46] Y.J.Pei[1] S.Pensotti[26] D.Perret-Gallix[4] A.Pevsner[5] D.Piccolo[28] M.Pieri[16] J.C.Pinto[34] P.A.Piroué[35] E.Pistolesi[16] V.Plyaskin[27] M.Pohl[46] V.Pojidaev[27,16] H.Postema[15] N.Produit[19] K.N.Qureshi[18] R.Raghavan[9] G.Rahal-Callot[46] P.G.Rancoita[26] M.Rattaggi[26] G.Raven[2] P.Razis[29] K.Read[31] M.Redaelli[26] D.Ren[46] Z.Ren[18] M.Rescigno[36] S.Reucroft[11] A.Ricker[1] S.Riemann[45] B.C.Riemers[43] K.Riles[3] O.Rind[3] H.A.Rizvi[18] S.Ro[41] A.Robohm[46] J.Rodin[15] F.J.Rodriguez[25] B.P.Roe[3] M.Röhner[1] S.Röhner[1] L.Romero[25] S.Rosier-Lees[4] Ph.Rosselet[22] W.van Rossum[2] S.Roth[1] J.A.Rubio[17] H.Rykaczewski[46] J.Salicio[17] J.M.Salicio[25] E.Sanchez[25] A.Santocchia[33] M.E.Sarakinos[21] S.Sarkar[9] G.Sartorelli[18] M.Sassowsky[1] G.Sauvage[4] C.Schäfer[1] V.Schegelsky[37] D.Schmitz[1] P.Schmitz[1] M.Schneegans[4] B.Schoeneich[45] N.Scholz[46] H.Schopper[47] D.J.Schotanus[30] R.Schulte[1] K.Schultze[1] J.Schwenke[1] G.Schwering[1] C.Sciacca[28] R.Sehgal[18] P.G.Seiler[44] J.C.Sens[48] L.Servoli[33] S.Shevchenko[32] N.Shivarov[40] V.Shoutko[27] J.Shukla[23] E.Shumilov[27] D.Son[41] A.Sopczak[17] V.Soulimov[28] B.Smith[15] T.Spickermann[1] P.Spillantini[16] M.Steuer[15] D.P.Stickland[35] F.Sticozzi[15] H.Stone[35] B.Stoyanov[40] K.Strauch[14] K.Sudhakar[9] G.Sultanov[18] L.Z.Sun[20,18] G.F.Susinno[19] H.Suter[46] J.D.Swain[18] A.A.Syed[30] X.W.Tang[6] L.Taylor[11] R.Timellini[8] Samuel C.C.Ting[15] S.M.Ting[15] O.Toker[33] M.Tonutti[1] S.C.Tonwar[9] J.Tóth[13] A.Tsaregorodtsev[37] G.Tsipolitis[34] C.Tully[35] H.Tuchscherer[42] J.Ulbricht[46] L.Urbán[13] U.Uwer[1] E.Valente[36] R.T.Van de Walle[30] I.Vetlitsky[27] G.Viertel[46] P.Vikas[18] U.Vikas[18] M.Vivargent[4] R.Voelkert[45] H.Vogel[34] H.Vogt[45] I.Vorobiev[27] A.A.Vorobyov[37] An.A.Vorobyov[37] L.Vuilleumier[22] M.Wadhwa[25] W.Wallraff[1] J.C.Wang[15] X.L.Wang[20] Y.F.Wang[15] Z.M.Wang[18,20] A.Weber[1] R.Weill[22] C.Willmott[25] F.Wittgenstein[17] S.X.Wu[18] S.Wynhoff[1] J.Xu[10] Z.Z.Xu[20] B.Z.Yang[20] C.G.Yang[6] G.Yang[18] X.Y.Yao[6] C.H.Ye[18] J.B.Ye[20] Q.Ye[18] S.C.Yeh[48] J.M.You[34] N.Yunus[18] M.Yzerman[2] C.Zaccardelli[32] An.Zalite[37] P.Zemp[46] J.Y.Zeng[6] M.Zeng[18] Y.Zeng[1] Z.Zhang[6] Z.P.Zhang[20,18] B.Zhou[10] G.J.Zhou[6] J.F.Zhou[1] Y.Zhou[3] G.Y.Zhu[6] R.Y.Zhu[32] A.Zichichi[8,17,18] B.C.C.van der Zwaan[2]

1 I. Physikalisches Institut, RWTH, D-52056 Aachen, FRG[§]
III. Physikalisches Institut, RWTH, D-52056 Aachen, FRG[§]
2 National Institute for High Energy Physics, NIKHEF, NL-1009 DB Amsterdam, The Netherlands
3 University of Michigan, Ann Arbor, MI 48109, USA
4 Laboratoire d'Annecy-le-Vieux de Physique des Particules, LAPP,IN2P3-CNRS, BP 110, F-74941 Annecy-le-Vieux CEDEX, France
5 Johns Hopkins University, Baltimore, MD 21218, USA
6 Institute of High Energy Physics, IHEP, 100039 Beijing, China
7 Humboldt University, D-10099 Berlin, FRG[§]
8 INFN-Sezione di Bologna, I-40126 Bologna, Italy
9 Tata Institute of Fundamental Research, Bombay 400 005, India
10 Boston University, Boston, MA 02215, USA
11 Northeastern University, Boston, MA 02115, USA
12 Institute of Atomic Physics and University of Bucharest, R-76900 Bucharest, Romania
13 Central Research Institute for Physics of the Hungarian Academy of Sciences, H-1525 Budapest 114, Hungary[‡]
14 Harvard University, Cambridge, MA 02139, USA
15 Massachusetts Institute of Technology, Cambridge, MA 02139, USA
16 INFN Sezione di Firenze and University of Florence, I-50125 Florence, Italy
17 European Laboratory for Particle Physics, CERN, CH-1211 Geneva 23, Switzerland
18 World Laboratory, FBLJA Project, CH-1211 Geneva 23, Switzerland
19 University of Geneva, CH-1211 Geneva 4, Switzerland
20 Chinese University of Science and Technology, USTC, Hefei, Anhui 230 029, China
21 SEFT, Research Institute for High Energy Physics, P.O. Box 9, SF-00014 Helsinki, Finland
22 University of Lausanne, CH-1015 Lausanne, Switzerland
23 Los Alamos National Laboratory, Los Alamos, NM 87544, USA
24 Institut de Physique Nucléaire de Lyon, IN2P3-CNRS,Université Claude Bernard, F-69622 Villeurbanne Cedex, France
25 Centro de Investigaciones Energeticas, Medioambientales y Tecnologicas, CIEMAT, E-28040 Madrid, Spain♭
26 INFN-Sezione di Milano, I-20133 Milan, Italy
27 Institute of Theoretical and Experimental Physics, ITEP, Moscow, Russia
28 INFN-Sezione di Napoli and University of Naples, I-80125 Naples, Italy
29 Department of Natural Sciences, University of Cyprus, Nicosia, Cyprus
30 University of Nymegen and NIKHEF, NL-6525 ED Nymegen, The Netherlands
31 Oak Ridge National Laboratory, Oak Ridge, TN 37831, USA
32 California Institute of Technology, Pasadena, CA 91125, USA
33 INFN-Sezione di Perugia and Universitá Degli Studi di Perugia, I-06100 Perugia, Italy
34 Carnegie Mellon University, Pittsburgh, PA 15213, USA
35 Princeton University, Princeton, NJ 08544, USA
36 INFN-Sezione di Roma and University of Rome, "La Sapienza", I-00185 Rome, Italy
37 Nuclear Physics Institute, St. Petersburg, Russia
38 University of California, San Diego, CA 92093, USA
39 Dept. de Fisica de Particulas Elementales, Univ. de Santiago, E-15706 Santiago de Compostela, Spain
40 Bulgarian Academy of Sciences, Central Laboratory of Mechatronics and Instrumentation, BU-1113 Sofia, Bulgaria
41 Center for High Energy Physics, Korea Advanced Inst. of Sciences and Technology, 305-701 Taejon, Republic of Korea
42 University of Alabama, Tuscaloosa, AL 35486, USA
43 Purdue University, West Lafayette, IN 47907, USA
44 Paul Scherrer Institut, PSI, CH-5232 Villigen, Switzerland
45 DESY-Institut für Hochenergiephysik, D-15738 Zeuthen, FRG
46 Eidgenössische Technische Hochschule, ETH Zürich, CH-8093 Zürich, Switzerland
47 University of Hamburg, D-22761 Hamburg, FRG
48 High Energy Physics Group, Taiwan, China
§ Supported by the German Bundesministerium für Bildung, Wissenschaft, Forschung und Technologie
‡ Supported by the Hungarian OTKA fund under contract number 2970.
♭ Supported also by the Comisión Interministerial de Ciencia y Technología
♯ Also supported by CONICET and Universidad Nacional de La Plata, CC 67, 1900 La Plata, Argentina

# References


[1] H. Fritzsch, M. Gell-Mann and H. Leytwyler, Phys. Lett. **B47** (1973) 365;
D. J. Gross and F. Wilczek, Phys. Rev. Lett. **30** (1973) 1343;
D. J. Gross and F. Wilczek, Phys. Rev. **8** (1973) 3633;
H. D. Politzer, Phys. Rev. Lett. **30** (1973) 1346.

[2] Yu. Dokshitzer, V. A. Khoze, S. I. Troyan and A. H. Mueller, Rev. Mod. Phys. **60** (1988) 373;
Yu. L. Dokshitzer, V. A. Khoze, A. H. Mueller and S. I. Troyan, *Basics of Perturbative QCD* (Editions Frontières, Paris) 1991.

[3] B. I. Ermolaev and V. S. Fadin, JETP Lett. **33** (1981) 269;
A. H. Mueller, Phys. Lett. **B 104** (1981) 161;
A. Bassetto, M. Ciafaloni, G. Marchesini and A. H. Mueller, Nucl. Phys. **B 207** (1982) 189;
G. Marchesini and B. R. Webber, Nucl. Phys. **B 238** (1984) 1-29.

[4] Ya. I. Azimov, Yu. L. Dokshitzer, V. A. Khoze and S. I. Troyan, Z. Phys. **C 27** (1985) 65.

[5] K. Konashi, A. Ukawa and G. Veneziano, Nucl. Phys. **B 157** (1979) 45;
G. Altarelli and G. Parisi, Nucl. Phys. **B 126** (1977) 298.

[6] T. Sjöstrand and M. Bengtsson, Computer Phys. Comm. **43** (1987) 367;
T. Sjöstrand, CERN preprint: CERN-TH.6488/92.

[7] G. Marchesini *et al.*, Computer Phys. Comm. **67** (1992) 465.

[8] L. Lönnblad, Computer Phys. Comm. **71** (1992) 15.

[9] R. Odorico, Computer Phys. Comm. **72** (1992) 235.

[10] R. K. Ellis, D. A. Ross, and A. E. Terrano, Nucl. Phys. **B 178** (1981) 421;
R.-Y. Zhu, Ph.D. thesis, M. I. T., MIT-LNS Report RX-1033 (1983); Cal. Tech. Report CALT-68-1306; in Proc. 1984 DPF Conf., Santa Fe, p. 229; in Proc. 1985 DPF Conf., Oregon, p. 552.

[11] Ya. I. Azimov, Yu. L. Dokshitzer, V. A. Khoze and S. I. Troyan, Phys. Lett. **B 165** (1985) 147.

[12] B. Andersson, G. Gustafson and T. Sjöstrand, Phys. Lett. **B 94** (1980) 211.

[13] JADE Collaboration, W. Bartel *et al.*, Phys. Lett. **B 101** (1981) 129.

[14] L3 Collaboration, M. Acciarri *et al.*, Phys. Lett. **B 345** (1995) 74.

[15] L3 Collaboration, M. Acciarri *et al.*, Phys. Lett. **B 328** (1994) 223.

[16] OPAL Collaboration, P. D. Acton *et al.*, Z. Phys. **C 58** (1993) 207.

[17] C. Louis Basham *et al.*, Phys. Rev. Lett. **41** (1978) 1585.

[18] A. Ali and F. Barrerio, Nucl. Phys. **B 236** (1984) 269.

[19] L3 Collaboration, B. Adeva *et al.*, Nucl. Instr. and Meth. **A 289** (1990) 35;
L3 Collaboration, O. Adriani *et al.*, Phys. Rep. **236** (1993) 1.

[20] Aly Aamer Syed, Ph.D. thesis, University of Nijmegen (1994), ISBN 90-9007038-9.

[21] L3 Collaboration, B. Adeva *et al.*, Z. Phys. **C 51** (1991) 179.

[22] L3 Collaboration, B. Adeva *et al.*, Z. Phys. **C 55** (1992) 39.

[23] G. Gustafson, G. Ingelman and T. Sjöstrand, Phys. Rep. **97** (1983) 31.

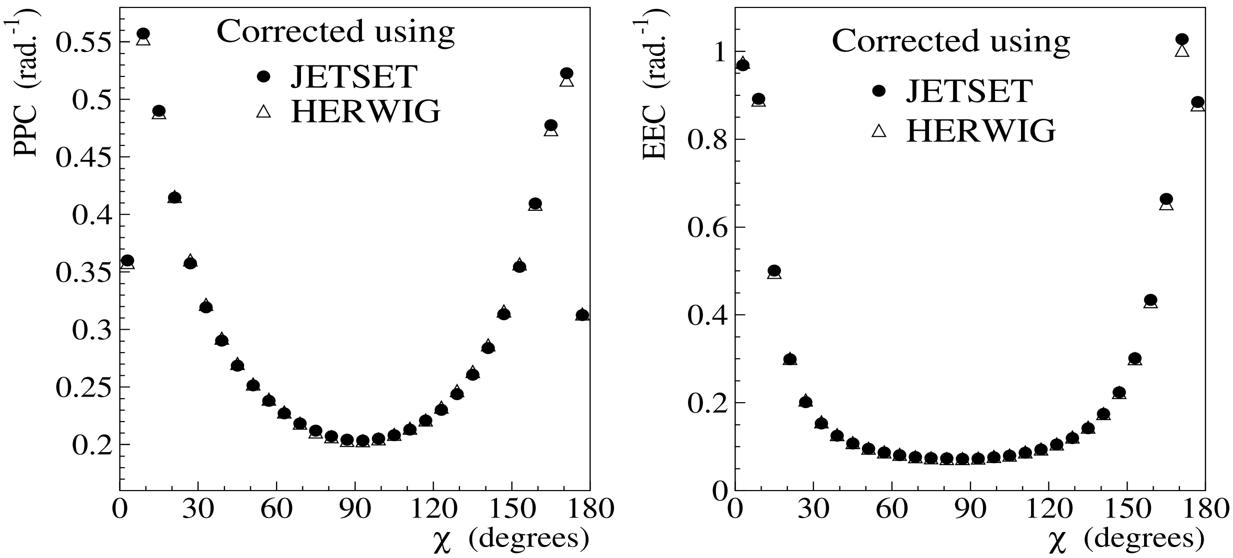


Figure 1: The PPC and EEC distributions of the data corrected using JETSET and HERWIG. Statistical errors are smaller than the points.

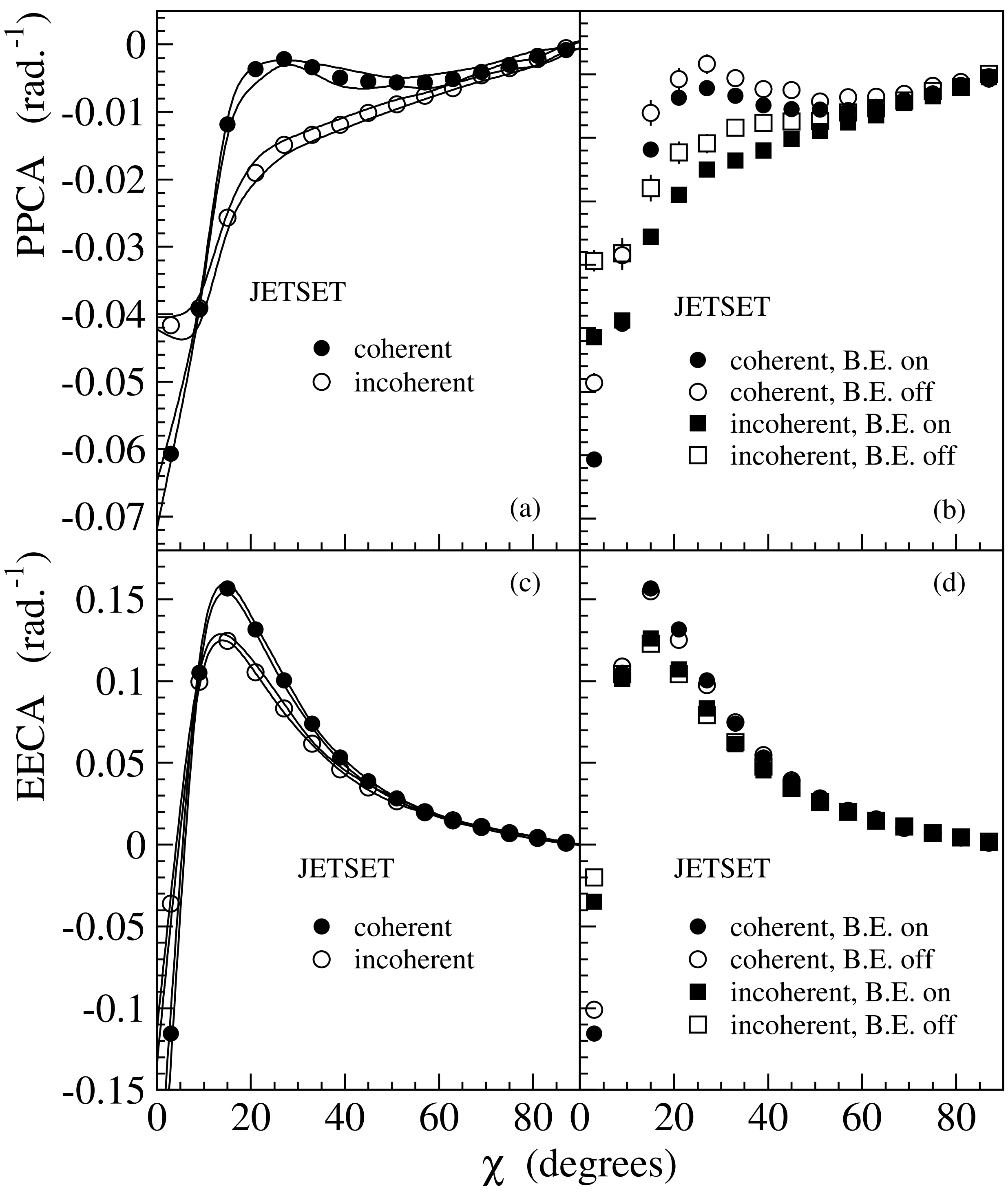


Figure 2: Dependence of (a) the PPCA and (c) the EECA on the JETSET parameters described in the text for the angular ordered and non-angular ordered case, and the dependence of (b) the PPCA and (d) EECA on the Bose-Einstein effect. The bands in (a) and (c) represent the maximum and minimum values found in varying the three parameters by $\pm 1$ standard deviation.

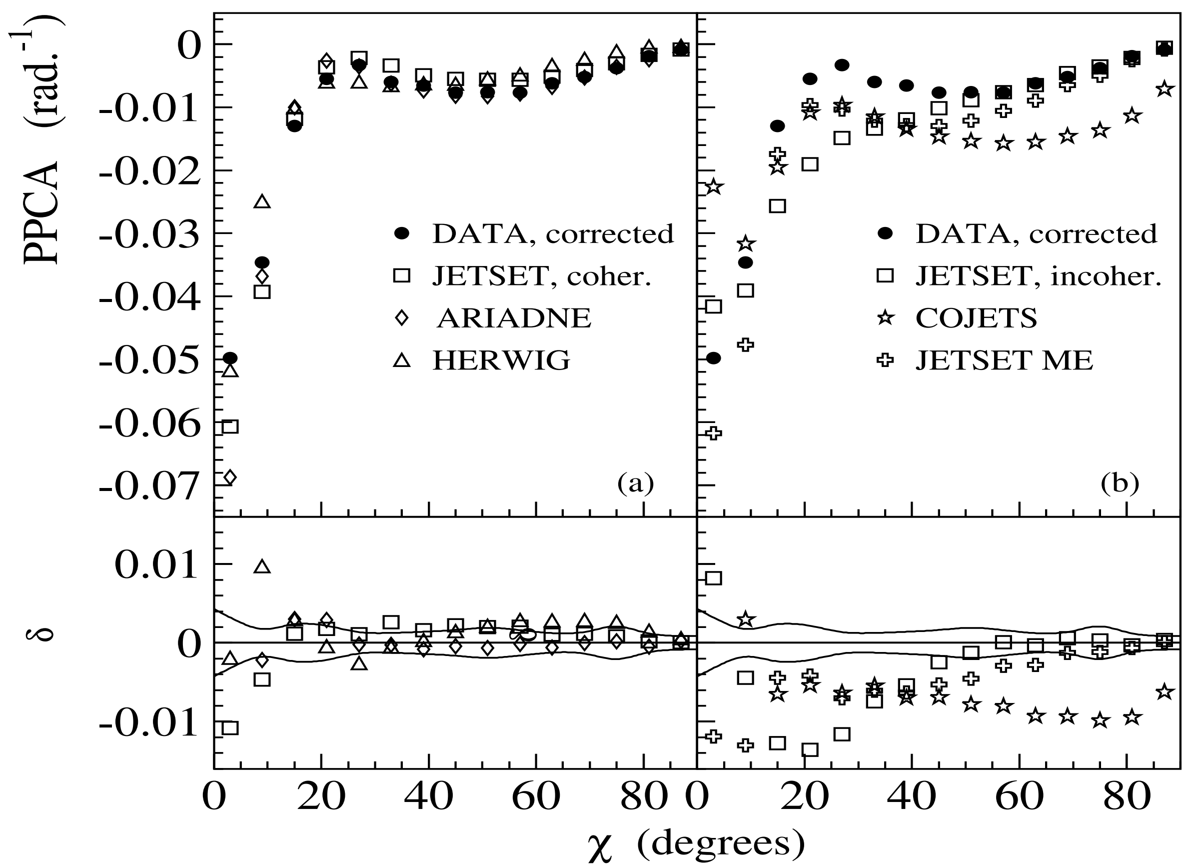


Figure 3: The corrected PPCA distributions compared to (a) coherent and (b) incoherent Monte Carlo models. The upper plots show the correlation asymmetries themselves; the lower plots show the differences, $\delta$, between the correlation asymmetries of the models and those of the data. Statistical errors on data and Monte Carlo are smaller than the points. The bands indicate statistical plus systematic errors from both model uncertainties and correction of the data for detector efficiency and resolution.

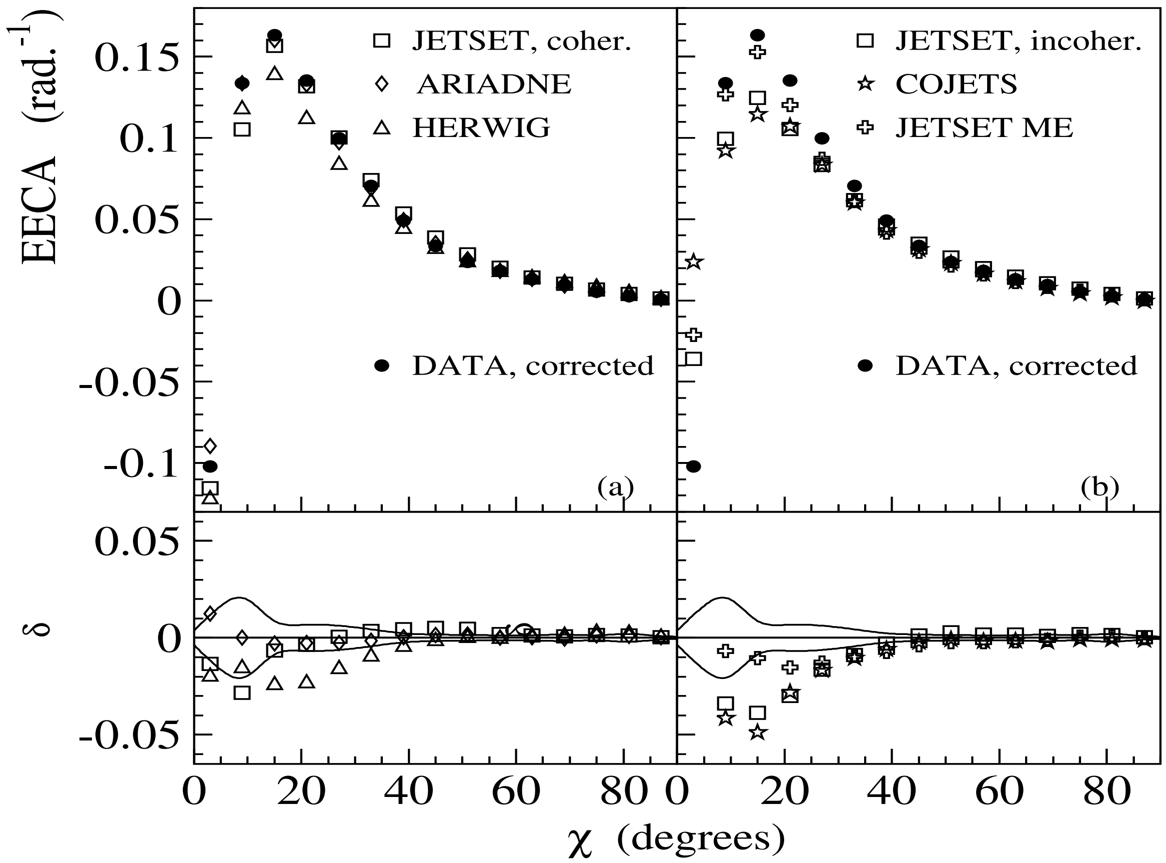


Figure 4: The corrected EECA distributions compared to (a) coherent and (b) incoherent Monte Carlo models. The upper plots show the correlation asymmetries themselves; the lower plots show the differences, $\delta$, between the correlation asymmetries of the models and those of the data. Statistical errors on data and Monte Carlo are smaller than the points. The bands indicate statistical plus systematic errors from both model uncertainties and correction of the data for detector efficiency and resolution.